







## Current experimental upper bounds on spacetime diffusion

Martijn Janse <sup>\*</sup>, Dennis G. Uitenbroek <sup>\*</sup>, Loek van Everdingen <sup>\*</sup>, Jaimy Plugge <sup>\*</sup>,  
 Bas Hensen <sup>†</sup> and Tjerk H. Oosterkamp <sup>‡</sup>  
*Leiden Institute of Physics, Leiden University, P.O. Box 9504, 2300 RA Leiden, The Netherlands*



(Received 8 March 2024; accepted 18 May 2024; published 17 July 2024)

A theory describing the dynamics of quantum systems interacting on a classical spacetime was recently put forward by Oppenheim *et al.* Quantum states may retain their coherence, at the cost of some amount of stochasticity of the spacetime metric, characterized by a spacetime diffusion parameter. Here, we report existing experimental upper bounds on such spacetime diffusion, based on a review of several types of experiments with very low force noise over a broad range of test masses from single atoms to several kilograms. We find an upper bound at least 15 orders of magnitude lower as compared to the initial bounds for explicit models presented by Oppenheim *et al.* The results presented here provide a path forward for future experiments that can help evaluate classical-quantum theories.

DOI: [10.1103/PhysRevResearch.6.033076](https://doi.org/10.1103/PhysRevResearch.6.033076)

### I. INTRODUCTION

Oppenheim *et al.* have pointed out that quantum mechanics can be combined with a classical interpretation of gravity, while limiting the amount of decoherence of quantum systems caused by the classical field [1,2]. To this end, they have introduced a spacetime diffusion parameter,  $D_2$ , which describes the fluctuations arising due to the interplay between a quantum system and its surrounding classical gravitational potential. Put differently, this is the rate of diffusion of the conjugate momenta of the Newtonian potential, which is necessary to preserve any amount of coherence of the quantum system subject to classical gravity.

Three different models were put forward in Oppenheim *et al.* [1] to describe this spacetime diffusion parameter, each with their own upper and lower bound. The ultralocal continuous model has already been ruled out in the original paper by comparison with experiments. However, the remaining two models, i.e., the ultralocal discrete and the nonlocal continuous model, are not yet rejected (Eqs. (46) and (47), respectively in Ref. [1]). In the ultralocal discrete model  $D_2$  has an upper bound of

$$\frac{l_p^3}{m_p} D_2 \leq \frac{\sigma_a^2 N \Delta T r_N^4}{m_N G^2} \quad (1)$$

and in the nonlocal continuous model  $D_2$  has an upper bound of

$$l_p^2 D_2 \leq \frac{\sigma_a^2 N \Delta T r_N^3}{G^2}. \quad (2)$$

Here,  $l_p$  is the Planck length,  $m_p$  the Planck mass,  $G$  the gravitational constant,  $r_N$  the radius of the nucleus, and  $m_N$  its mass. In addition to this upper bound, Oppenheim *et al.* also introduce a lower bound based on decoherence experiments. We do not address this lower bound extensively in this work. In order for the theory to be ruled out in the current formulation, there are still 26 and 24 orders of magnitude of  $D_2$  to be overcome in the ultralocal discrete model and the nonlocal continuous model, respectively.

Leaving the natural constants aside and assuming the radius and mass of the nucleus to be constant in the experiment we consider, we find three parameters that combine in the same way for both expressions. These are the acceleration noise  $\sigma_a$ , the number of nuclei  $N$ , and the measurement time  $\Delta T$ . These three parameters essentially introduce a figure of merit  $\text{FOM}_{D_2}$ , which needs to be minimized in order for the upper bound on  $D_2$  to be lowered for both models. The  $\text{FOM}_{D_2}$  may be deduced from precision experiments that minimize acceleration and/or force noise

$$\text{FOM}_{D_2} = \sigma_a^2 N \Delta T = S_a N. \quad (3)$$

Here, we use the spectral density  $S_a = \sigma_a^2 \Delta T$ . To facilitate the comparison with different experiments, we prefer to use the spectral densities  $S_a$  rather than the variance  $\sigma_a^2$ , such that the measurement time  $\Delta T$  drops out of the equations. Since many experiments focus on the force noise,  $S_F$ , rather than the acceleration noise, it is necessary to convert  $S_a$  to  $S_F$ , using  $\sigma_F = m \sigma_a$  or  $S_F = m^2 S_a$ . The mass  $m = MN/N_A$  is related to the number of particles  $N$  through the average molar mass  $M$  of the materials used and Avogadro's number  $N_A$ . In the case of molecules, we multiply the number of particles  $N$  by the number of nuclei per molecule.

<sup>\*</sup>These authors share first authorship and contributed equally to this paper.

<sup>†</sup>Contact author: [hensen@physics.leidenuniv.nl](mailto:hensen@physics.leidenuniv.nl)

<sup>‡</sup>Contact author: [oosterkamp@physics.leidenuniv.nl](mailto:oosterkamp@physics.leidenuniv.nl)

Published by the American Physical Society under the terms of the [Creative Commons Attribution 4.0 International](https://creativecommons.org/licenses/by/4.0/) license. Further distribution of this work must maintain attribution to the author(s) and the published article's title, journal citation, and DOI.

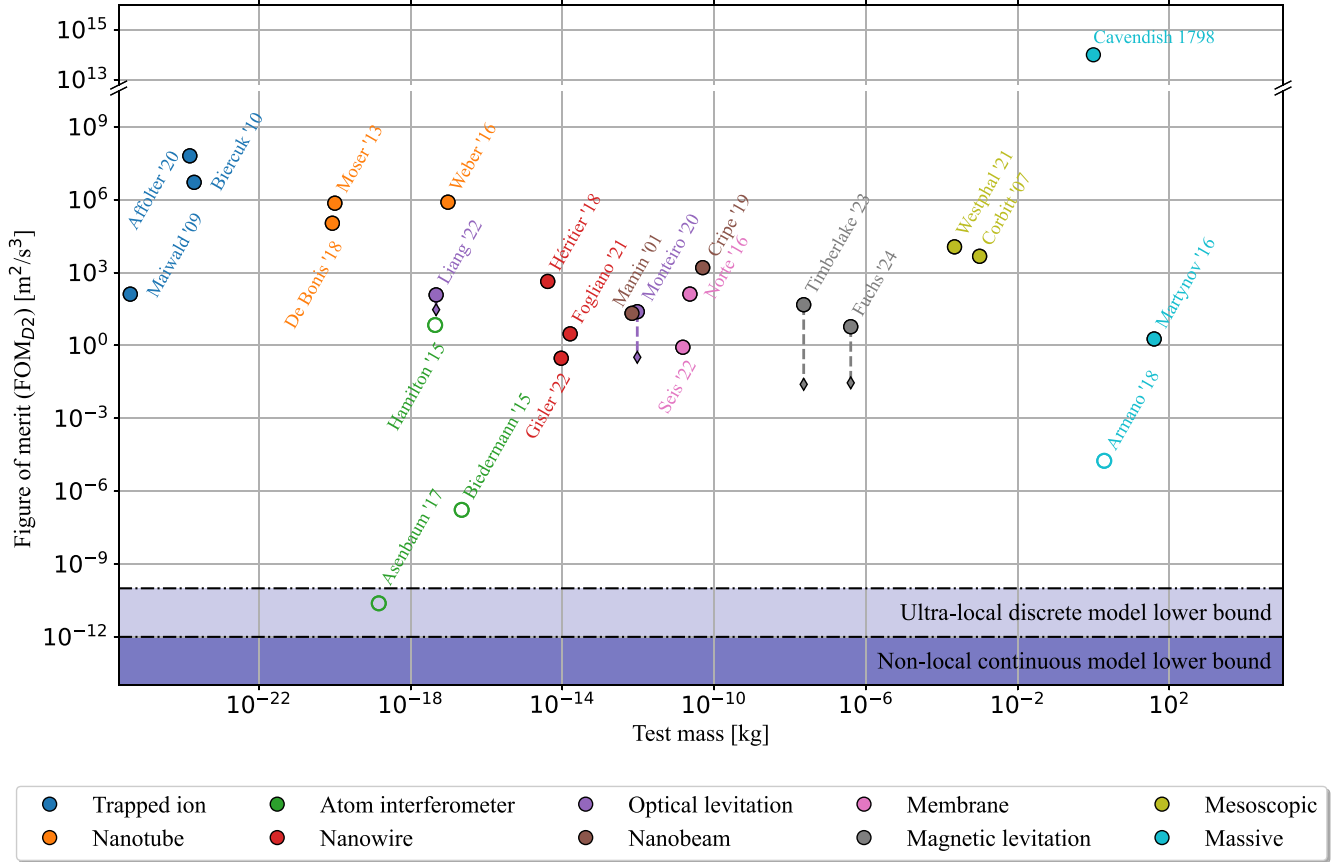


FIG. 1. The figure of merit  $FOM_{D_2}$  as calculated for different kind of force sensitivity experiments. Different types of experiments along a broad mass range were considered. Plotted experiments are considered to be representative of their type. The actual measurement reported for each experiment is plotted as a circle. A diamond, indicating a potential thermal force limit, is added to experiments in which the total force noise is at least two times larger than the thermal force noise. Markers with a colored edge indicate that the experiment was a differential measurement and therefore the validity of the calculated  $FOM_{D_2}$  is questioned. The shaded areas in the bottom part of the plot indicate the lower bound that was put on  $FOM_{D_2}$  by Oppenheim *et al.* for respectively the ultralocal discrete model and the nonlocal continuous model.

In this work we point out that the figure of merit for modern-day experiments, ranging from atom interferometry to the LISA Pathfinder mission, can vastly outperform the figure of merit of the Cavendish torsion balance experiment, which Oppenheim *et al.* used as a first source of experimental bound on their models [1]. For this first bound, Oppenheim *et al.* used  $N = 10^{26}$ ,  $\sigma_a = 10^{-7} \text{ m/s}^2$ , and  $\Delta T = 100 \text{ s}$ , leading to  $FOM_{D_2} = 10^{14} \text{ m}^2/\text{s}^3$ .

## II. RESULTS

In Fig. 1 we show  $FOM_{D_2}$  as a function of the test mass for different types of experiments with low force or acceleration noise. The underlying data is shown in Table I in Appendix. We observe that experiments with test masses in the range between  $10^{-22} \text{ kg}$  and  $10^2 \text{ kg}$  can yield a stronger upper bound compared to the Cavendish torsion balance experiment. An experiment by Gisler *et al.* [3] achieves a  $FOM_{D_2}$  that is 15 orders of magnitude lower by using a nanowire mechanical resonator with an effective mass of  $9.3 \times 10^{-15} \text{ kg}$ . This measurement results in the lowest  $FOM_{D_2}$  with an absolute measurement of acceleration noise on Earth. A slightly higher  $FOM_{D_2}$  is achieved by Martynov *et al.* [4], which concerns

the LIGO mirror with a test mass of several kilograms. This is an indication that the minimal achievable acceleration noise is largely independent of the test mass.

On top of that, we also observe an improvement of 19 orders of magnitude for Armano *et al.* [5], i.e., the LISA Pathfinder mission to explore in-space detection of gravitational waves. In this experiment a displacement is measured by means of a laser interferometric arm. However, this concerns a differential acceleration noise measurement and is in that sense a relative measurement instead of an absolute measurement of the acceleration noise. This may have implications for the applicability of these experimental results to bound the models. Furthermore, in their derivation, Oppenheim *et al.* note that the bound on  $D_2$  will depend on the functional choice of  $D_2(\Phi)$  on the Newtonian potential  $\Phi$ , for which they assume that of a large background potential, i.e., that of the Earth. However, the LISA Pathfinder measurement is done very far away from the Earth, at its Lagrange point  $L_1$ . This may affect the validity of this  $FOM_{D_2}$  calculation.

In terms of  $FOM_{D_2}$ , atom interferometry experiments outperform all other types of experiments: Asenbaum *et al.* [6] improve the  $FOM_{D_2}$  by 25 orders of magnitude in comparison to the Cavendish experiment put forward in the original paper

TABLE I. Overview of all experiments that were considered in this paper. Note that not all experiments presented in this table are plotted in Fig. 1. For each experiment the measured parameters relevant for calculating the figure of merit,  $FOM_{D_2}$ , are shown. The columns in this table contain from left to right: a reference to the original paper, the type of experiment, the material of the mechanical oscillator, the test mass  $m$ , the number of nuclei  $N$ , the resonance frequency  $f_0$ , the total force noise  $S_F$ , the acceleration noise  $S_a$  and the figure of merit  $FOM_{D_2}$  of the experiment. (†) If a value in the table was unavailable in the original paper, we report the value mentioned in the review paper. (\*) The material described is borosilicate glass. We assumed this to consist for 80% of  $SiO_2$  and for 20% of  $B_2O_3$ .

Reference	Type	Element	$m$ [kg]	$N$ [-]	$f_0$ [Hz]	$\sqrt{S_F}$ [N/ $\sqrt{Hz}$ ]	$\sqrt{S_a}$ [ms $^{-2}$ / $\sqrt{Hz}$ ]	$FOM_{D_2}$ [ $m^2 s^{-3}$ ]
Asenbaum '17 [6]	Atom interfer.	Rb	$1.44 \times 10^{-19}$	$1.00 \times 10^6$	-	$7.08 \times 10^{-28}$	$4.91 \times 10^{-9}$	$2.41 \times 10^{-11}$
Biedermann '15 [22]	Atom interfer.	Cs	$2.21 \times 10^{-17}$	$1.00 \times 10^8$	-	$9.09 \times 10^{-25}$	$4.12 \times 10^{-8}$	$1.70 \times 10^{-7}$
Armano '18 [5]	Massive	Au	1.93	$5.89 \times 10^{24}$	-	$3.35 \times 10^{-15}$	$1.74 \times 10^{-15}$	$1.78 \times 10^{-5}$
Gisler '22 [3]	Nanowire	$Si_3N_4$	$9.30 \times 10^{-15}$	$2.79 \times 10^{11}$	$1.41 \times 10^6$	$9.60 \times 10^{-21}$	$1.03 \times 10^{-6}$	$2.98 \times 10^{-1}$
Seis '22 [23]	Membrane	$Si_3N_4$	$1.50 \times 10^{-11}$	$4.51 \times 10^{14}$	$1.49 \times 10^6$	$6.50 \times 10^{-19}$	$4.33 \times 10^{-8}$	$8.46 \times 10^{-1}$
Martynov '16 [4,18]†	Massive	$SiO_2$	$4.00 \times 10^1$	$1.20 \times 10^{27}$	$1.00 \times 10^2$	$1.57 \times 10^{-12}$	$3.92 \times 10^{-14}$	1.85
Fogliano '21 [24]	Nanowire	SiC	$1.60 \times 10^{-14}$	$4.82 \times 10^{11}$	$1.16 \times 10^4$	$4.00 \times 10^{-20}$	$2.50 \times 10^{-6}$	3.01
Fuchs '24 [8]	Magnetic lev.	$Nd_2Fe_{14}B$	$4.00 \times 10^{-7}$	$3.79 \times 10^{18}$	$2.67 \times 10^1$	$5.00 \times 10^{-16}$	$1.25 \times 10^{-9}$	5.92
Hamilton '15 [25]	Atom interfer.	Cs	$4.41 \times 10^{-18}$	$2.00 \times 10^7$	-	$2.60 \times 10^{-21}$	$5.89 \times 10^{-4}$	6.93
Mamin '01 [26]	Nanobeam	Si	$6.85 \times 10^{-13}$	$1.47 \times 10^{13}$	$4.98 \times 10^3$	$8.20 \times 10^{-19}$	$1.20 \times 10^{-6}$	$2.11 \times 10^1$
Monteiro '20 [27]	Optical lev.	$SiO_2$	$9.42 \times 10^{-13}$	$2.84 \times 10^{13}$	$6.30 \times 10^1$	$8.78 \times 10^{-19}$	$9.32 \times 10^{-7}$	$2.46 \times 10^1$
Timberlake '23 [9]	Magnetic lev.	$Nd_2Fe_{14}B$	$2.30 \times 10^{-8}$	$2.18 \times 10^{17}$	$4.24 \times 10^1$	$3.40 \times 10^{-16}$	$1.48 \times 10^{-8}$	$4.76 \times 10^1$
Liang '22 [20]	Optical lev.	$SiO_2$	$4.68 \times 10^{-18}$	$1.41 \times 10^8$	$1.75 \times 10^5$	$4.34 \times 10^{-21}$	$9.27 \times 10^{-4}$	$1.21 \times 10^2$
Maiwald '09 [28]	Trapped ion	$Mg^+$	$4.04 \times 10^{-26}$	1.00	$1.00 \times 10^6$	$4.60 \times 10^{-25}$	$1.14 \times 10^1$	$1.30 \times 10^2$
Norte '16 [29]	Membrane	$Si_3N_4$	$2.30 \times 10^{-11}$	$6.91 \times 10^{14}$	$1.50 \times 10^5$	$1.00 \times 10^{-17}$	$4.35 \times 10^{-7}$	$1.31 \times 10^2$
Kampel '17 [18,30]†	Membrane	$Si_3N_4$	$1.00 \times 10^{-11}$	$3.00 \times 10^{14}$	$1.60 \times 10^6$	$9.81 \times 10^{-18}$	$9.81 \times 10^{-7}$	$2.89 \times 10^2$
Héritier '18 [31]	Nanowire	C	$4.10 \times 10^{-15}$	$2.06 \times 10^{11}$	$2.50 \times 10^4$	$1.88 \times 10^{-19}$	$4.59 \times 10^{-5}$	$4.33 \times 10^2$
Tebbenjohanns '20 [20,32]†	Optical lev.	$SiO_2$	$3.49 \times 10^{-18}$	$1.05 \times 10^8$	$1.46 \times 10^5$	$8.00 \times 10^{-21}$	$2.29 \times 10^{-3}$	$5.52 \times 10^2$
Tebbenjohanns '19 [20,33]†	Optical lev.	$SiO_2$	$3.49 \times 10^{-18}$	$1.05 \times 10^8$	$1.46 \times 10^5$	$1.00 \times 10^{-20}$	$2.87 \times 10^{-3}$	$8.63 \times 10^2$
Lewandowski '21 [34]	Magnetic lev.	$SiO_2, B_2O_3^*$	$2.50 \times 10^{-10}$	$8.26 \times 10^{15}$	1.75	$8.83 \times 10^{-17}$	$3.53 \times 10^{-7}$	$1.03 \times 10^3$
Teufel '09 [35]	Nanowire	Al	$5.50 \times 10^{-15}$	$1.23 \times 10^{11}$	$1.04 \times 10^6$	$5.10 \times 10^{-19}$	$9.27 \times 10^{-5}$	$1.05 \times 10^3$
Cripe '19 [18,36]†	Nanobeam	GaAs	$5.00 \times 10^{-11}$	$4.16 \times 10^{14}$	$8.76 \times 10^2$	$9.81 \times 10^{-17}$	$1.96 \times 10^{-6}$	$1.60 \times 10^3$
Reinhardt '16 [37]	Membrane	$Si_3N_4$	$4.00 \times 10^{-12}$	$1.20 \times 10^{14}$	$4.08 \times 10^4$	$2.00 \times 10^{-17}$	$5.00 \times 10^{-6}$	$3.00 \times 10^3$
Gieseler '13 [38]	Optical lev.	$SiO_2$	$3.00 \times 10^{-18}$	$9.03 \times 10^7$	$1.25 \times 10^5$	$2.00 \times 10^{-20}$	$6.67 \times 10^{-3}$	$4.01 \times 10^3$
Delić '20 [39]	Optical lev.	$SiO_2$	$2.83 \times 10^{-18}$	$8.52 \times 10^7$	$3.05 \times 10^5$	$1.94 \times 10^{-20}$	$6.87 \times 10^{-3}$	$4.02 \times 10^3$
Corbitt '07 [40]	Mesoscopic	$SiO_2$	$1.00 \times 10^{-3}$	$3.01 \times 10^{22}$	$1.80 \times 10^3$	$3.95 \times 10^{-13}$	$3.95 \times 10^{-10}$	$4.70 \times 10^3$
Westphal '21 [41]	Mesoscopic	Au	$2.18 \times 10^{-4}$	$6.66 \times 10^{20}$	$3.59 \times 10^{-3}$	$9.07 \times 10^{-13}$	$4.16 \times 10^{-9}$	$1.15 \times 10^4$
Rider '18 [42]	Optical lev.	$SiO_2$	$1.53 \times 10^{-13}$	$4.62 \times 10^{12}$	$2.50 \times 10^2$	$1.15 \times 10^{-17}$	$7.50 \times 10^{-5}$	$2.60 \times 10^4$
Kawasaki '20 [43]	Optical lev.	$SiO_2$	$8.40 \times 10^{-14}$	$2.53 \times 10^{12}$	$3.01 \times 10^2$	$1.00 \times 10^{-17}$	$1.19 \times 10^{-4}$	$3.58 \times 10^4$
Hempston '17 [44]	Optical lev.	$SiO_2$	$7.60 \times 10^{-19}$	$2.29 \times 10^7$	$7.20 \times 10^4$	$3.20 \times 10^{-20}$	$4.21 \times 10^{-2}$	$4.06 \times 10^4$
De Bonis '18 [19]	Nanotube	C	$8.60 \times 10^{-21}$	$4.32 \times 10^5$	$2.92 \times 10^7$	$4.30 \times 10^{-21}$	$5.00 \times 10^{-1}$	$1.08 \times 10^5$
Hälg '21 [45]	Membrane	$Si_3N_4$	$1.40 \times 10^{-11}$	$4.21 \times 10^{14}$	$1.42 \times 10^6$	$2.80 \times 10^{-16}$	$2.00 \times 10^{-5}$	$1.68 \times 10^5$
Priel '22 [46]	Optical lev.	$SiO_2$	$5.85 \times 10^{-13}$	$1.76 \times 10^{13}$	$1.00 \times 10^5$	$1.00 \times 10^{-16}$	$1.71 \times 10^{-4}$	$5.14 \times 10^5$
Moser '13 [47]	Nanotube	C	$1.00 \times 10^{-20}$	$5.02 \times 10^5$	$4.20 \times 10^6$	$1.20 \times 10^{-20}$	1.20	$7.23 \times 10^5$
Weber '16 [48]	Nanotube	C	$9.60 \times 10^{-18}$	$4.82 \times 10^8$	$4.60 \times 10^7$	$3.90 \times 10^{-19}$	$4.06 \times 10^{-2}$	$7.95 \times 10^5$
Ranjit '16 [49]	Optical lev.	$SiO_2$	$3.75 \times 10^{-17}$	$1.13 \times 10^9$	$2.83 \times 10^3$	$1.63 \times 10^{-18}$	$4.35 \times 10^{-2}$	$2.14 \times 10^6$
Krause '12 [50]	Membrane	$Si_3N_4$	$1.00 \times 10^{-11}$	$3.00 \times 10^{14}$	$2.75 \times 10^4$	$9.81 \times 10^{-16}$	$9.81 \times 10^{-5}$	$2.89 \times 10^6$
Nichol '12 [51]	Nanowire	Si	$2.66 \times 10^{-17}$	$5.72 \times 10^8$	$7.86 \times 10^5$	$1.95 \times 10^{-18}$	$7.33 \times 10^{-2}$	$3.07 \times 10^6$
Biercuk '10 [52]	Trapped ion	$Be^+$	$1.95 \times 10^{-24}$	$1.30 \times 10^2$	$8.67 \times 10^5$	$3.90 \times 10^{-22}$	$2.00 \times 10^2$	$5.22 \times 10^6$
Ranjit '15 [53]	Optical lev.	$SiO_2$	$3.75 \times 10^{-14}$	$1.13 \times 10^{12}$	$1.07 \times 10^3$	$2.17 \times 10^{-16}$	$5.79 \times 10^{-3}$	$3.78 \times 10^7$
Affolter '20 [54]	Trapped ion	$Be^+$	$1.50 \times 10^{-24}$	$1.00 \times 10^2$	$1.58 \times 10^6$	$1.20 \times 10^{-21}$	$8.02 \times 10^2$	$6.43 \times 10^7$
Timberlake '19 [55]	Magnetic lev.	$Nd_2Fe_{14}B$	$4.00 \times 10^{-6}$	$3.79 \times 10^{19}$	$1.94 \times 10^1$	$7.85 \times 10^{-12}$	$1.96 \times 10^{-6}$	$1.46 \times 10^8$
Guzmán C. '14 [56]	Mesoscopic	$SiO_2$	$2.50 \times 10^{-5}$	$7.53 \times 10^{20}$	$1.07 \times 10^4$	$2.45 \times 10^{-11}$	$9.81 \times 10^{-7}$	$7.24 \times 10^8$
Shaniv '17 [57]	Trapped ion	$Sr^+$	$1.44 \times 10^{-25}$	1.00	$1.13 \times 10^6$	$2.80 \times 10^{-20}$	$1.94 \times 10^5$	$3.78 \times 10^{10}$
Blums '18 [58]	Trapped ion	$Yb^+$	$2.89 \times 10^{-25}$	1.00	$8.29 \times 10^5$	$3.47 \times 10^{-19}$	$1.20 \times 10^6$	$1.44 \times 10^{12}$
Cavendish 1798 [59]	Massive	Pb	1.00	$1.00 \times 10^{26}$	$2.00 \times 10^{-3}$	$1.00 \times 10^{-6}$	$1.00 \times 10^{-6}$	$1.00 \times 10^{14}$

by Oppenheim *et al.* and the  $FOM_{D_2}$  even drops below the lower bound of the ultralocal discrete model describing the spacetime diffusion. However, the value is still one order of magnitude larger than the limit set by the nonlocal continuous model. We note that this experiment is qualitatively different from the Cavendish torsion balance experiments in the sense

that a phase shift is measured instead of a displacement. This is a relative measurement of the acceleration noise and as such the same considerations apply as for the experiment by Armano *et al.* [5]. Lastly, although an acceleration sensitivity is measured in the atom interferometer, we are unsure to which extent its results are valid to calculate the upper bound. After

all, these atom interferometry experiments closely resemble the matter-wave interferometry experiment that Oppenheim *et al.* use to set a lower bound based on decoherence experiments [7]. It raises the question if one and the same experiment can put both an upper and a lower bound on  $D_2$ .

We point out that several low-force noise measurements on Earth can still be improved, such as magnets levitating in a superconducting well making use of the Meissner effect, reported by Fuchs *et al.* [8] and Timberlake *et al.* [9]. These experiments measure force sensitivity by means of yet another technique, namely Superconducting Quantum Interference Devices (SQUID) detection. This type of experiment is currently not limited by thermal noise. Further improvements in vibration isolation will help to close the gap to the thermal noise floor, potentially outperforming the LIGO mirror.

### III. DISCUSSION

We consider a broad range of experiments to lay a solid foundation for a new upper bound to the spacetime diffusion parameter  $D_2$  that is at least 15 orders of magnitude better than the first bound provided in the original paper. Experiments for which the applicability of the results to this upper bound calculation are questioned are indicated with an open marker in Fig. 1. Inclusion of these experiments can improve the upper bound by up to 25 orders of magnitude, thus dropping below the bound set by the ultralocal discrete model. Furthermore, we would like to point out that, using the experimental results of Asenbaum *et al.*, there is still a gap of one order of magnitude (out of 26 orders of magnitude) that needs to be closed for the nonlocal continuous model.

A class of experiments worth mentioning are those investigating the nature of spacetime [10–12]. These experiments aim to study hypothetical deviations from our current interpretation of general relativity, such as a variable speed of light and deviations from the local position invariance principle. A more thorough analysis of the theory put forward by Oppenheim *et al.* is necessary to assess the consequences of these experiments on its validity. The implications cannot readily be related to the used definition of  $FOM_{D_2}$  in this work, since it does not necessarily involve a measurement of force or acceleration noise. As such, they fall outside the scope of this paper.

Additionally, it is important to realize that we have only considered an improvement of the upper bound on the spacetime diffusion parameter in this work. Oppenheim *et al.* calculate the lower limit on  $D_2$ , set by coherence measurements of large-mass quantum superposition states, from interferometry experiments showing coherent quantum interference of fullerene molecules [7]. Although we have not elaborately reviewed experimental results of coherence measurements, we argue that this lower bound may be raised by examining more novel experiments. For instance, Fein *et al.* [13] present an updated result of the matter-wave interferometry experiment, which Oppenheim *et al.* put forward as a first lower bound, where the mass in superposition now exceeds 25 kDa and the decoherence rate is given by  $\lambda = \tau^{-1} = 133$  Hz. Next, Wang *et al.* [14] report the coherence of a  $^{171}\text{Yb}^+$  ion qubit with a decoherence rate of  $\lambda = 182$   $\mu\text{Hz}$ . However, the superposed state in question is a spin

superposition and thus not a mass displacement superposition. Lastly, Bild *et al.* [15] show a cat state of a 16  $\mu\text{g}$  mechanical oscillator with a decoherence rate of  $\lambda \sim 1$  MHz. Closer examination of these decoherence experiments may result in new insights on the lower bound on  $D_2$ .

Examining a broad range of modern-day experiments over a large test mass range allows us to lower the upper bound on the spacetime diffusion parameter  $D_2$ . If only direct measurements of acceleration sensitivity on Earth are considered, i.e., excluding the open data points in Fig. 1, the updated bounds become

$$10^{-16} \geq \frac{l_P^3}{m_P} D_2 \geq 10^{-25} \quad (4)$$

for the ultralocal discrete model and

$$10^{-24} \geq l_P^2 D_2 \geq 10^{-35} \quad (5)$$

for the nonlocal continuous model. Here we report a conservative bound. More in-depth scrutiny of the theory put forward by Oppenheim *et al.* should provide a better understanding of the applicability of the atom interferometry and LISA Pathfinder experimental results.

In order to discuss future improvements of  $FOM_{D_2}$ , the origin of the force noise in the experiments in Fig. 1 is considered. We distinguish between thermal force noise  $S_F^{\text{th}}$  and other noise sources. The former can be expressed as

$$S_F^{\text{th}} = 4k_B T m \gamma = 4k_B T m \omega_0 / Q \quad (6)$$

with  $T$  the mode temperature and  $\gamma$  the damping coefficient of the oscillating mode of the test mass. Furthermore, the resonance frequency is denoted as  $\omega_0$  and the quality factor is denoted as  $Q$  for the oscillating mode. An experiment is considered to be thermally limited if the thermal force noise  $S_F^{\text{th}}$  is larger than half the measured total force noise  $S_F$ . This distinction is made since thermal force noise has a lower limit set by the fluctuation-dissipation theorem. The  $FOM_{D_2}$  calculated from only the thermal force noise of an experiment is plotted in Fig. 1 if it is at least a factor of two lower than the  $FOM_{D_2}$  calculated from the measured total force noise. This is the case for at least four experiments for which the force or acceleration sensitivity is measured directly. Other sources of force noise generally originate from imperfections in the measurement setup, such as insufficient vibration isolation.

Assuming an experiment is thermally limited, we have  $FOM_{D_2} = 4Nk_B T \omega_0 / (mQ) \sim T \omega_0 / Q$ . This relation shows that lowering the test mass  $m$  is not necessary to improve the  $FOM_{D_2}$ , as also becomes clear from Fig. 1. However, this relation indicates that the parameters  $T$ ,  $\omega_0$  and  $Q$  can be used to lower the thermal noise floor. Lowering the temperature  $T$  of an experiment often requires drastic changes to the experimental setup, such as carrying out the experiment inside a dilution refrigerator or using vibration isolation systems [16]. The parameter  $Q$  is related to the amount of damping in a mechanical oscillator. Improving the  $FOM_{D_2}$  in terms of damping would require improved fabrication of the, often nanomechanical, oscillator. This is generally the preferred direction for improving force-sensitivity experiments, as is reflected in the recent development of a broad range of high- $Q$  resonators [17]. In terms of the resonance frequency  $\omega_0$  we observe for the reviewed experiments that the  $FOM_{D_2}$  is slightly better

for experiments with a lower  $\omega_0$ . Lowering the resonance frequency  $\omega_0$  of an experiment also comes with technical challenges, as vibration isolation at ever lower frequencies becomes increasingly difficult.

Summarizing, several of the presented experiments pave the way to further limit the bounds they put on the spacetime diffusion parameter. We look forward to further discussions on the validity of the upper bounds provided by the atom interferometry and LISA Pathfinder experiments, as well as other ways to evaluate the theory for the spacetime diffusion parameter put forward by Oppenheim *et al.*

#### ACKNOWLEDGMENTS

We thank P. Logman and G. van de Stolpe for their contributions to the manuscript. This work was supported by the European Union (ERC StG, CLOSEtoQG, Project No. 101041115), the EU Horizon Europe EIC Pathfinder project QuCoM (10032223) and the NWO Grant No. OCENW.GROOT.2019.088.

#### APPENDIX: OVERVIEW OF EXPERIMENTS

For this paper we have reviewed a broad range of different experimental platforms that aim to measure force or acceleration with ultrahigh sensitivity. These include (mechanical) resonators with high quality factors that, for instance, make use of soft clamping or levitation. Other types of experiments are more mesoscopic or macroscopic (massive), such as modern-day torsion pendula and the latest vibration-isolated platforms employed by the LIGO and LISA Pathfinder collaboration. Yet another type of experiment that we have included are atom interferometry measurements. These are qualitatively different in the sense that they measure a phase shift

instead of a displacement, but provide nonetheless very precise acceleration measurements.

We have included measurements of force or acceleration sensitivity that are actual experimental results (as opposed to theoretically achievable values). These include, for example, measurements with SQUIDs or laser interferometry. We have not included papers that only report experimental results of, e.g., displacement of strain sensitivity measurements (as opposed to force or acceleration sensitivity), although we think that these measurements could also give potentially interesting results for  $FOM_{D_2}$ . In order to find relevant papers, we thankfully consulted previous reviews on precision force-sensitivity measurements [17–21].

Based on test mass magnitude, fabrication technique, and measurement method, we distinguish ten different types of experiments. They are clustered as follows:

(i) suspended systems: (carbon) nanotubes, nanowires (e.g., suspended SiC or Al wires), nanobeams (e.g., GaAs or single-crystal Si cantilevers), SiN membranes, mesoscopic (e.g., milligram torsion pendulum), and massive (e.g., the LIGO mirror),

(ii) levitated systems: trapped ion, optical levitation (e.g., silica nanobeads in optical tweezers), and magnetic levitation (e.g., magnets in superconducting wells),

(iii) free-falling systems: atom interferometry.

For every category, the two or three experiments that gave the best  $FOM_{D_2}$  were plotted in Fig. 1. To calculate  $FOM_{D_2}$ , we have looked up the element and mass of the test mass, from which we could derive the number of nuclei. Additionally, we listed the spectral density of the force and acceleration sensitivity. These values are also listed in Table I. If available in the paper and applicable to the experiment, we have also looked up the resonance frequency, quality factors, mode temperatures, and damping coefficient in order to be able to calculate the thermal noise floor via Eq. (6).

- 
- [1] J. Oppenheim, C. Sparaciari, B. Šoda, and Z. Weller-Davies, Gravitationally induced decoherence vs space-time diffusion: testing the quantum nature of gravity, *Nat. Commun.* **14**, 7910 (2023).
- [2] J. Oppenheim, A postquantum theory of classical gravity, *Phys. Rev. X* **13**, 041040 (2023).
- [3] T. Gisler, M. Helal, D. Sabonis, U. Grob, M. H eritier, C. L. Degen, A. H. Ghadimi, and A. Eichler, Soft-clamped silicon nitride string resonators at millikelvin temperatures, *Phys. Rev. Lett.* **129**, 104301 (2022).
- [4] D. Martynov, E. D. Hall *et al.*, Sensitivity of the advanced ligo detectors at the beginning of gravitational wave astronomy, *Phys. Rev. D* **93**, 112004 (2016).
- [5] M. Armano *et al.*, Beyond the required lisa free-fall performance: New LISA pathfinder results down to 20  $\mu$ Hz, *Phys. Rev. Lett.* **120**, 061101 (2018).
- [6] P. Asenbaum, C. Overstreet, T. Kovachy, D. D. Brown, J. M. Hogan, and M. A. Kasevich, Phase shift in an atom interferometer due to spacetime curvature across its wave function, *Phys. Rev. Lett.* **118**, 183602 (2017).
- [7] S. Gerlich, S. Eibenberger, M. Tomandl, S. Nimmrichter, K. Hornberger, P. J. Fagan, J. T uxen, M. Mayor, and M. Arndt, Quantum interference of large organic molecules, *Nat. Commun.* **2**, 263 (2011).
- [8] T. M. Fuchs, D. G. Uitenbroek, J. Plugge, N. V. Halteren, P. V. Soest, A. Vinante, H. Ulbricht, and T. H. Oosterkamp, Measuring gravity with milligram levitated masses, *Sci. Adv.* **10**, 8 (2024).
- [9] C. Timberlake, E. Simcox, and H. Ulbricht, Linear cooling of a levitated micromagnetic cylinder by vibration, [arXiv:2310.03880](https://arxiv.org/abs/2310.03880).
- [10] J. Magueijo, New varying speed of light theories, *Rep. Prog. Phys.* **66**, 2025 (2003).
- [11] N. Ashby, T. E. Parker, and B. R. Patla, A null test of general relativity based on a long-term comparison of atomic transition frequencies, *Nat. Phys.* **14**, 822 (2018).
- [12] S. Herrmann, F. Finke, M. L ulf, O. Kichakova, D. Puetzfeld, D. Knickmann, M. List, B. Rievers, G. Giorgi, C. G unther *et al.*, Test of the gravitational redshift with *Galileo* satellites in an eccentric orbit, *Phys. Rev. Lett.* **121**, 231102 (2018).
- [13] Y. Y. Fein, P. Geyer, P. Zwick, F. Kialka, S. Pedalino, M. Mayor, S. Gerlich, and M. Arndt, Quantum superposition of molecules beyond 25 kDa, *Nat. Phys.* **15**, 1242 (2019).

- [14] P. Wang, C. Y. Luan, M. Qiao, M. Um, J. Zhang, Y. Wang, X. Yuan, M. Gu, J. Zhang, and K. Kim, Single ion qubit with estimated coherence time exceeding one hour, *Nat. Commun.* **12**, 233 (2021).
- [15] M. Bild, M. Fadel, Y. Yang, U. V. Lüpke, P. Martin, A. Bruno, and Y. Chu, Schrödinger cat states of a 16-microgram mechanical oscillator, *Science* **380**, 274 (2023).
- [16] M. D. Wit, G. Welker, K. Heeck, F. M. Buters, H. J. Eerkens, G. Koning, H. V. der Meer, D. Bouwmeester, and T. H. Oosterkamp, Vibration isolation with high thermal conductance for a cryogen-free dilution refrigerator, *Rev. Sci. Instrum.* **90**, 015112 (2019).
- [17] A. Eichler, Ultra-high- $Q$  nanomechanical resonators for force sensing, *Mater. Quantum Technol.* **2**, 043001 (2022).
- [18] D. Carney, G. Krnjaic, D. C. Moore, C. A. Regal, G. Afek, S. Bhave, B. Brubaker, T. Corbitt, J. Cripe, N. Crisosto, A. Geraci, S. Ghosh, J. G. Harris, A. Hook, E. W. Kolb, J. Kunjummen, R. F. Lang, T. Li, T. Lin, Z. Liu *et al.*, Mechanical quantum sensing in the search for dark matter, *Quantum Sci. Technol.* **6**, 024002 (2021).
- [19] S. L. D. Bonis, C. Urgell, W. Yang, C. Samanta, A. Noury, J. Vergara-Cruz, Q. Dong, Y. Jin, and A. Bachtold, Ultrasensitive displacement noise measurement of carbon nanotube mechanical resonators, *Nano Lett.* **18**, 5324 (2018).
- [20] T. Liang, S. Zhu, P. He, Z. Chen, Y. Wang, C. Li, Z. Fu, X. Gao, X. Chen, N. Li, Q. Zhu, and H. Hu, Yoctonewton force detection based on optically levitated oscillator, *Fund. Res.* **3**, 57 (2023).
- [21] D. C. Moore and A. A. Geraci, Searching for new physics using optically levitated sensors, *Quantum Sci. Technol.* **6**, 014008 (2021).
- [22] G. W. Biedermann, X. Wu, L. Deslauriers, S. Roy, C. Mahadeswaraswamy, and M. A. Kasevich, Testing gravity with cold-atom interferometers, *Phys. Rev. A* **91**, 033629 (2015).
- [23] Y. Seis, T. Capelle, E. Langman, S. Saarinen, E. Planz, and A. Schliesser, Ground state cooling of an ultracoherent electromechanical system, *Nat. Commun.* **13**, 1507 (2022).
- [24] F. Fogliano, B. Besga, A. Reigue, L. M. de Lépinay, P. Heringlake, C. Gouriou, E. Eyraud, W. Wernsdorfer, B. Pigeau, and O. Arcizet, Ultrasensitive nano-optomechanical force sensor operated at dilution temperatures, *Nat. Commun.* **12**, 4124 (2021).
- [25] P. Hamilton, M. Jaffe, J. M. Brown, L. Maisenbacher, B. Estey, and H. Müller, Atom interferometry in an optical cavity, *Phys. Rev. Lett.* **114**, 100405 (2015).
- [26] H. J. Mamin and D. Rugar, Sub-atto-newton force detection at millikelvin temperatures, *Appl. Phys. Lett.* **79**, 3358 (2001).
- [27] F. Monteiro, W. Li, G. Afek, C. L. Li, M. Mossman, and D. C. Moore, Force and acceleration sensing with optically levitated nanogram masses at microkelvin temperatures, *Phys. Rev. A* **101**, 053835 (2020).
- [28] R. Maiwald, D. Leibfried, J. Britton, J. C. Bergquist, G. Leuchs, and D. J. Wineland, Stylus ion trap for enhanced access and sensing, *Nat. Phys.* **5**, 551 (2009).
- [29] R. A. Norte, J. P. Moura, and S. Gröblacher, Mechanical resonators for quantum optomechanics experiments at room temperature, *Phys. Rev. Lett.* **116**, 147202 (2016).
- [30] N. S. Kampel, R. W. Peterson, R. Fischer, P. L. Yu, K. Cicak, R. W. Simmonds, K. W. Lehnert, and C. A. Regal, Improving broadband displacement detection with quantum correlations, *Phys. Rev. X* **7**, 021008 (2017).
- [31] M. Héritier, A. Eichler, Y. Pan, U. Grob, I. Shorubalko, M. D. Krass, Y. Tao, and C. L. Degen, Nanoladder cantilevers made from diamond and silicon, *Nano Lett.* **18**, 1814 (2018).
- [32] F. Tebbenjohanns, M. Frimmer, V. Jain, D. Windey, and L. Novotny, Motional sideband asymmetry of a nanoparticle optically levitated in free space, *Phys. Rev. Lett.* **124**, 013603 (2020).
- [33] F. Tebbenjohanns, M. Frimmer, A. Militaru, V. Jain, and L. Novotny, Cold damping of an optically levitated nanoparticle to microkelvin temperatures, *Phys. Rev. Lett.* **122**, 223601 (2019).
- [34] C. W. Lewandowski, T. D. Knowles, Z. B. Etienne, and B. D'Urso, High-sensitivity accelerometry with a feedback-cooled magnetically levitated microsphere, *Phys. Rev. Appl.* **15**, 014050 (2021).
- [35] J. D. Teufel, T. Donner, M. A. Castellanos-Beltran, J. W. Harlow, and K. W. Lehnert, Nanomechanical motion measured with an imprecision below that at the standard quantum limit, *Nat. Nanotechnol.* **4**, 820 (2009).
- [36] J. Cripe, N. Aggarwal, R. Lanza, A. Libson, R. Singh, P. Heu, D. Follman, G. D. Cole, N. Mavalvala, and T. Corbitt, Measurement of quantum back action in the audio band at room temperature, *Nature (London)* **568**, 364 (2019).
- [37] C. Reinhardt, T. Müller, A. Bourassa, and J. C. Sankey, Ultralow-noise sin trampoline resonators for sensing and optomechanics, *Phys. Rev. X* **6**, 021001 (2016).
- [38] J. Gieseler, L. Novotny, and R. Quidant, Thermal nonlinearities in a nanomechanical oscillator, *Nat. Phys.* **9**, 806 (2013).
- [39] U. Delić, M. Reisenbauer, K. Dare, D. Grass, V. Vuletić, N. Kiesel, and M. Aspelmeyer, Cooling of a levitated nanoparticle to the motional quantum ground state, *Science* **367**, 892 (2020).
- [40] T. Corbitt, Y. Chen, E. Innerhofer, H. Müller-Ebhardt, D. Ottaway, H. Rehbein, D. Sigg, S. Whitcomb, C. Wipf, and N. Mavalvala, An all-optical trap for a gram-scale mirror, *Phys. Rev. Lett.* **98**, 150802 (2007).
- [41] T. Westphal, H. Hepach, J. Pfaff, and M. Aspelmeyer, Measurement of gravitational coupling between millimetre-sized masses, *Nature (London)* **591**, 225 (2021).
- [42] A. D. Rider, C. P. Blakemore, G. Gratta, and D. C. Moore, Single-beam dielectric-microsphere trapping with optical heterodyne detection, *Phys. Rev. A* **97**, 013842 (2018).
- [43] A. Kawasaki, A. Fieguth, N. Priel, C. P. Blakemore, D. Martin, and G. Gratta, High sensitivity, levitated microsphere apparatus for short-distance force measurements, *Rev. Sci. Instrum.* **91**, 083201 (2020).
- [44] D. Hempston, J. Vovrosh, M. Toroš, G. Winstone, M. Rashid, and H. Ulbricht, Force sensing with an optically levitated charged nanoparticle, *Appl. Phys. Lett.* **111**, 133111 (2017).
- [45] D. Hälgl, T. Gisler, Y. Tsaturyan, L. Catalini, U. Grob, M. D. Krass, M. Héritier, H. Mattiat, A. K. Thamm, R. Schirhagl, E. C. Langman, A. Schliesser, C. L. Degen, and A. Eichler, Membrane-based scanning force microscopy, *Phys. Rev. Appl.* **15**, L021001 (2021).
- [46] N. Priel, A. Fieguth, C. P. Blakemore, E. Hough, A. Kawasaki, D. Martin, G. Venugopalan, and G. Gratta, Dipole moment background measurement and suppression for levitated charge sensors, *Sci. Adv.* **8**, eabo2361 (2022).
- [47] J. Moser, J. Güttinger, A. Eichler, M. J. Esplandiú, D. E. Liu, M. I. Dykman, and A. Bachtold, Ultrasensitive force detection

- with a nanotube mechanical resonator, *Nat. Nanotechnol.* **8**, 493 (2013).
- [48] P. Weber, J. Güttinger, A. Noury, J. Vergara-Cruz, and A. Bachtold, Force sensitivity of multilayer graphene optomechanical devices, *Nat. Commun.* **7**, 12496 (2016).
- [49] G. Ranjit, M. Cunningham, K. Casey, and A. A. Geraci, Zep-tonewton force sensing with nanospheres in an optical lattice, *Phys. Rev. A* **93**, 053801 (2016).
- [50] A. G. Krause, M. Winger, T. D. Blasius, Q. Lin, and O. Painter, A high-resolution microchip optomechanical accelerometer, *Nat. Photon.* **6**, 768 (2012).
- [51] J. M. Nichol, E. R. Hemesath, L. J. Lauhon, and R. Budakian, Nanomechanical detection of nuclear magnetic resonance using a silicon nanowire oscillator, *Phys. Rev. B* **85**, 054414 (2012).
- [52] M. J. Biercuk, H. Uys, J. W. Britton, A. P. Vandevender, and J. J. Bollinger, Ultrasensitive detection of force and displacement using trapped ions, *Nat. Nanotechnol.* **5**, 646 (2010).
- [53] G. Ranjit, D. P. Atherton, J. H. Stutz, M. Cunningham, and A. A. Geraci, Attonewton force detection using microspheres in a dual-beam optical trap in high vacuum, *Phys. Rev. A* **91**, 051805(R) (2015).
- [54] M. Affolter, K. A. Gilmore, J. E. Jordan, and J. J. Bollinger, Phase-coherent sensing of the center-of-mass motion of trapped-ion crystals, *Phys. Rev. A* **102**, 052609 (2020).
- [55] C. Timberlake, G. Gasbarri, A. Vinante, A. Setter, and H. Ulbricht, Acceleration sensing with magnetically levitated oscillators above a superconductor, *Appl. Phys. Lett.* **115**, 224101 (2019).
- [56] F. G. Cervantes, L. Kumanchik, J. Pratt, and J. M. Taylor, High sensitivity optomechanical reference accelerometer over 10 kHz, *Appl. Phys. Lett.* **104**, 221111 (2014).
- [57] R. Shaniv and R. Ozeri, Quantum lock-in force sensing using optical clock doppler velocimetry, *Nat. Commun.* **8**, 14157 (2017).
- [58] V. Blūms, M. Piotrowski, M. I. Hussain, B. G. Norton, S. C. Connell, S. Gensemer, M. Lobino, and E. W. Streed, A single-atom 3D sub-attonewton force sensor, *Sci. Adv.* **4**, eaao4453 (2018).
- [59] H. Cavendish, Experiments to determine the density of the Earth, *Phil. Trans. R. Soc.* **88**, 469 (1798).